Simultaneous Current and Distant Electric Field Waveforms from Upward Lightning: Effect of Ionospheric Reflection

M. Azadifar[1], D. Li[1,2], F. Rachidi[1], M. Rubinstein[3], G. Diendorfer[4],
H. Pichler[4], M. Paolone[5] , and D. Pavanello[6]

1 Swiss Federal Institute of Technology, EMC Laboratory, Lausanne, Switzerland
2 Nanjing University of Information Science and Technology (NUIST), Nanjing, China
3 University of Applied Sciences of Western Switzerland, Yverdon, Switzerland
4 OVE Service GmbH, Dept. ALDIS, Vienna, Austria
5 Swiss Federal Institute of Technology, DESL Laboratory, Lausanne, Switzerland
6 University of Applied Sciences of Western Switzerland, Sion, Switzerland
mohammad.azadifar@epfl.ch

Abstract— **We present simultaneous current and wideband electric field waveforms at 380 km associated with upward flashes initiated from the Säntis Tower. To the best of the authors' knowledge, the presented dataset in this study includes the first simultaneous records of lightning currents and associated fields featuring ionospheric reflections, and the longest distance at which lightning fields have been measured simultaneously with the current. Electric field data are used to evaluate ionospheric reflection characteristics during day and night times using the so-called zero-zero and peak-peak methods. During daytime, the estimates for the ionospheric reflection height is about 80 km, corresponding to the D layer. The estimated height at night time is about 90 km, corresponding to the E layer. Finally, we present a full-wave, finite-difference time-domain (FDTD) analysis of the field propagation including the effect of the ionospheric reflection and compare the results with experimental data.**

Keywords— Ionospheric reflection; Lightning current; Electric field; FDTD simulation

I.   INTRODUCTION

The radiated electromagnetic field from distant lightning flashes constitutes a valuable source of information in the study of the properties of the ionosphere. Low frequency (ELF and VLF) electromagnetic field observations have been widely used to examine ionospheric reflection characteristics and various numerical approaches have been proposed to model lightning-ionosphere interaction (e.g., [*Inan et al.*, 2012]).

In this paper, we present simultaneous current and wideband electric field waveforms at 380 km distance from the strike point associated with upward flashes initiated from the Säntis Tower

(Appenzell, Northeastern Switzerland) which were recorded from April to October 2014.

The majority of the recorded electric field waveforms of individual strokes and ICC pulses feature one or two secondary overshoots which are inferred to be due to ionospheric reflections (e.g., [*Haddad et al.*, 2012]). To the best of the authors' knowledge, the presented dataset in this study represents the first simultaneous records of lightning currents and associated fields featuring ionospheric reflections. Simultaneous records of lightning currents and electromagnetic fields have been obtained using either triggered lightning or instrumented towers and reported in the literature. However, to the best of our knowledge, the longest distance at which fields have been measured simultaneously with the current is about 100 km for the Gaisberg Tower [*Diendorfer et al.*, 2014]. The field measurements at 380 km in the present paper represent, therefore, the longest distance at which electric fields from lightning have been measured simultaneously with the lightning current.

Finally, a full-wave, finite-difference time-domain (FDTD) analysis [*Cummer*, 2000, *Jacobson et al.*, 2009] of the field propagation including the effect of the ionospheric reflection is presented and compared with the experimental data. The reported data in this study can also be used to validate available methods to infer characteristics of ionospheric reflection (e.g., [*Cummer*, 2000, *Jacobson et al.*, 2009].

II.   MEASUREMENT SYSTEM

The Säntis Tower was instrumented in May 2010 for the measurement of lightning current parameters [*Romero et al.*, 2012]. The lightning current waveforms and their time-

derivatives are measured at two heights along the tower, 24 m and 82 m. More details on the measurement sensors and instrumentation system can be found in [*Romero et al.*, 2012, *Romero et al.*, 2013]. In 2013-2014, a certain number of updates were made to the overall measuring system, which are described in [*Azadifar et al.*, 2014].

Electric fields were measured at 380 km (Neudorf, Northern Austria) using a flat plate antenna [*Pichler et al.*, 2010]. The measured signal was digitized with a sampling rate of 5 MS/s. The integrator decay time constant was 0.5 ms, corresponding to a lower cutoff frequency of about 300 Hz. The Säntis triggering signal was sent to the field measurement station using TCP/IP over the internet. More information on the Neudorf measuring station can be found in [*Pichler et al.*, 2010].

III. DATA

During the period of analysis (April-October 2014), simultaneous records of currents and electric fields at 380 km were obtained for 29 flashes recorded at the Säntis Tower. Among the 29 flashes, 4 were classified as upward bipolar and 25 as negative upward events.

In this paper, we present an analysis of 11 negative upward flashes which contain 76 detectable current pulses (return strokes and fast ICC pulses) featuring secondary overshoots above the noise level in the electric field records which are inferred to be due to ionospheric reflections (the so-called sky-waves). Seven pulses occurred during daytime and 69 during nighttime.

Figure 1 presents simultaneous records of the overall waveforms of current and E-field associated with an upward negative flash occurred on 21 October 2014, at 20:23:22. Note that the current waveform contains 5 return strokes. The return strokes follow an ICC which has not been shown in the figure.
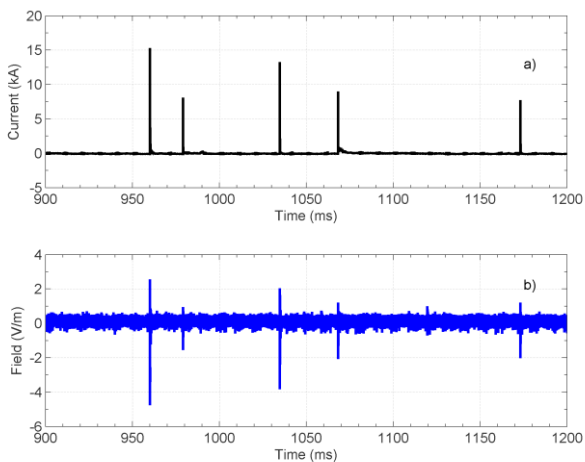

Fig. 1. Waveforms associated with an upward negative flash occurred on 21 October 2014 at 20:23:22. (a) Current waveform. (b) E-field waveform at 380 km.

Fig. 2 presents the waveforms associated with an individual return stroke in that flash. The current (Fig. 2a) is characterized by a peak value of 15.3 kA, a risetime of 1.6 μs and an FWHM (Full-Width Half-Maximum) of 57 μs. The field (Fig. 2b) is

characterized by an initial main pulse of about 4.7 V/m peak (ground wave), followed by two secondary overshoots occurring about 155 and 487 μs later. These overshoots are interpreted as being due to ionospheric reflections (sky-waves). It is worth noting that the fields at Neudorf are affected by a local enhancement factor of about 2.5 [Pichler et al., 2010]. The propagation paths of the ground wave and sky-waves are schematically represented in Fig. 3.
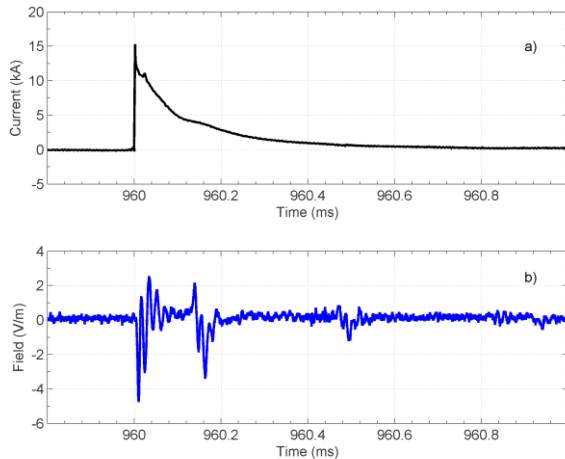

Fig. 2. Waveforms associated with the first return stroke of the upward negative flash of Fig. 2. (a) Current waveform. (b) E-field waveform at 380 km.
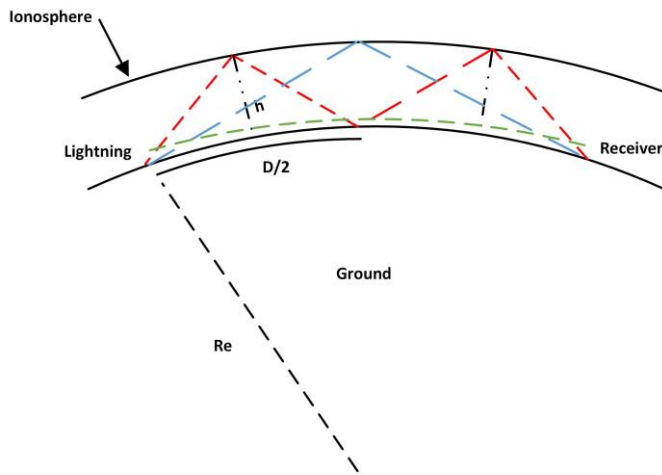

Fig. 3. Schematic representation of the propagation paths of the ground and sky-waves (the ground wave path is presented in Green.The first and second sky-waves are represented, respectively, in blue and in red).

IV. ANALYSIS

A. Height of the Ionospheric Reflection

Electric field data were used to evaluate ionospheric reflection characteristics during day and night times using the so-called zero-zero and peak-peak methods [*Haddad et al.*, 2012, *Somu et al.*, 2012]. Specifically, the ionospheric reflection height was determined using the following expression (used also

in *Haddad et al.* [2012]) which was obtained assuming the geometry of the path represented in blue in Fig. 3c:

$$h_1 = R_e \left[\cos(\frac{D}{2R_e}) - 1 \right] + \sqrt{\left\{ R_e^2 \left[\cos^2(\frac{D}{2R_e}) - 1 \right] + \left(\frac{ct_1 + D}{2} \right)^2 \right\}} \quad (1)$$

in which

- h_1 is the height of the ionospheric reflection. The subscript 1 refers to the fact that the equation uses the first skywave to infer this height;

- D is the distance from the lightning channel and the observation point (380 km);

- $R_e = 6367$ km is the mean radius of the Earth;

- c is the speed of light; and

- t_1 is the zero-to-zero or peak-to-peak time between the ground wave and the first skywave.

Table I presents the resulting arithmetic mean of the height of the ionospheric reflection, determined separately for daytime and night time.

TABLE I. ARITHMETIC MEAN OF THE HEIGHT OF THE IONOSPHERIC REFLECTION INFERRED FROM (1).

	Number of samples	Height of the ionospheric reflection (km)	
		using peak-to-peak time	using zero-to-zero time
Day time	7	78	76
Night time	69	91	89

It can be seen that, during daytime, the estimates for the ionospheric reflection height is about 76 to 78 km, corresponding to the D layer. As expected, the estimated height at night time increases to about 90 km, corresponding to the E layer.

Among the 76 simultaneous recorded pulses, 14 of them featured a second ionospheric reflection above the noise level of the field measuring system. All of these pulses occurred during nighttime which was expected due to lower attenuation of the D layer [*Nickolaenko et al.*, 2002]. Similar to Equation (1), it is straightforward to derive the following equation to derive the height of the ionospheric reflection using the second skywave (red path in Fig. 3c):

$$h_2 = R_e \times \left[\cos(\frac{D}{4R_e}) - 1 \right] + \sqrt{\left\{ R_e^2 \times \left[\cos^2(\frac{D}{4R_e}) - 1 \right] + \left(\frac{ct_1 + D}{4} \right)^2 \right\}} \quad (2)$$

Table 2 presents the arithmetic mean for the derived ionospheric reflection height using Equation (2). The results are also compared with the heights estimated using Equation (1) for the same set. It can be seen that the estimates obtained using Equation (2) are in better agreement with those of Equation (1) when the zero-to-zero time is used. This can be explained by the fact that the peak-to-peak times are largely affected by dispersion effects.

TABLE II. COMPARISON BETWEEN ARITHMETIC MEANS OF THE HEIGHT OF THE IONOSPHERIC REFLECTION INFERRED FROM (1) AND (2). ALL THE PULSES OCCURRED DURING NIGHT TIME.

	Number of samples	Height of the ionospheric reflection (km)	
		using peak-to-peak time	using zero-to-zero time
Eq. (1)	14	93	90
Eq. (2)	14	90	89

B. FDTD Simulation

Lightning electromagnetic fields were evaluated using spherical coordinates, within a two dimensional (2D) computational domain lying on the plane defined by the center of the Earth, the tower base and the field measurement point [*Bérenger*, 2002, *Thévenot and Bérenger*,1999]. Figure 4 shows the computational domain and the grid layout used in the model. The working space of the 2D FDTD is 400 km × 90 km, which is divided into 30-m quadrilateral cells. The time increment is set to 50 ns. In order to avoid reflections at the outer boundaries, we implemented the first-order Mur absorbing boundary conditions [*Mur*,1981]. The lightning channel was set in the symmetry axis of the model and the current distribution along the return stroke channel was specified according to the modified transmission line model with exponential decay (MTLE) [*Nucci et al.*, 1988; *Rachidi and Nucci*, 1990], assuming a current decay constant $\lambda = 2$ km [*Nucci and Rachidi*, 1989]. The measured channel base current waveform was represented using the sum of two Heidler's functions [*Heidler*, 1985], the parameters of which were determined using a Genetic Algorithm approach [*Bermudez et al.*, 2002].

The height of the ionosphere h is assmued to be 90 km, based on the inferred values (Table II). The height of the lightning channel was assumed to be $H = 7.5$ km, and the return stroke speed was set to v=1.5×10^8 m/s. The earth and the ionosphere were respectively characterized by a conductivity $\sigma_g = 10^{-3}$ S/m and $\sigma_i = 10^{-5}$ S/m. The relative permittivity was assumed to be 10 for both the earth and the ionosphere. Note finally that the presence of the tower and the mountain was not considered in the simulations.

Fig. 5 presents a comparison between the FDTD simulation results and the obtained experimental data for the measured waveforms of Fig. 2. It can be seen that the FDTD model allows to reproduce accurately the arrival times associated with the first and second sky-waves. However, the measured E-field signal features higher magnitudes. The disagreement can be explained, at least in part, by the enhancement of the fields due to the measurement arrangement at the observation site and due to the influence of the tower [*Rachidi et al.*, 2007].

Furthermore, a 60-kHz ringing can also be seen on the measured waveform whose origin is currently unknown. It is worth noting that similar ringing, but with lower amplitudes, can be observed in E-field waveforms reported in [*Jacobson et al.*, 2007; *Shao et al.*, 2013].
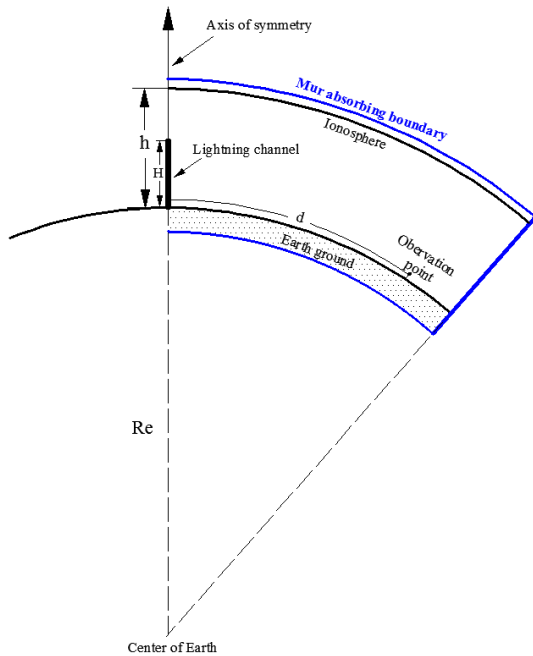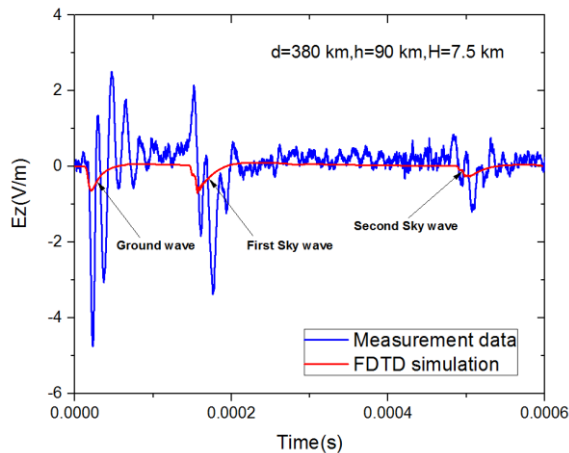

Fig. 4.   FDTD simulation domain.

Fig. 5.   FDTD simulations of the electomagnetic fields at 380 km, taking into account the ionospheric reflections and comparison with measured waveform.

V.   SUMMARY AND CONCLUSION

We presented simultaneous current and wideband electric field waveforms at 380 km associated with upward flashes initiated from the Säntis Tower. To the best of our knowledge, the presented dataset in this study includes the first simultaneous records of lightning currents and associated fields featuring ionospheric reflections, and the longest distance at which lightning fields have been measured simultaneously with the current.

The obtained electric field data were used to evaluate ionospheric reflection characteristics during day and night times using the so-called zero-zero and peak-peak methods. During daytime, the estimates for the ionospheric reflection height is about 76 to 78 km, corresponding to the D layer. The estimated height at night time is about 90 km, corresponding to the E layer.

Finally, we presented a full-wave, finite-difference time-domain (FDTD) analysis of the field propagation including the effect of the ionospheric reflection and found that the model reproduces satisfactorily the times of occurrence of the one-hop and the 2-hop sky waves, although the simulations appear to underestimate the amplitudes. The disagreement can be explained, at least in part, by the enhancement of the fields due to the measurement arrangement at the field observation site and due to the influence of the tower.

REFERENCES

Azadifar .M, M. Paolone, D. Pavanello, F. Rachidi, C. Romero, and M. Rubinstein (2014), "An Update on the Instrumentation of the Säntis Tower in Switzerland for Lightning Current Measurements and Obtained Results," in CIGRE International Colloquium on Lightning and Power Systems.

Bérenger, J. P. (2002). FDTD computation of VLF-LF propagation in the Earth-ionosphere waveguide. In Annales des télécommunications, Vol. 57, No. 11-12, pp. 1059-1090. Springer-Verlag.

Bermudez, J., C. Pena-Reyes, F. Rachidi, and F. Heidler (2002), "Use of genetic algorithms to extract primary lightning current parameters," in *Proceedings of EMC Europe 2002. International Symposium on Electromagnetic Compatibility*.

Cummer, S.A. (2000), Modeling electromagnetic propagation in the earth-ionosphere waveguide, IEEE Transactions on Antennas and Propagation, Vol. 48, No. 9, pp. 1420-1429.

Diendorfer, G., H. Zhou, H. Pichler, R. Thottappillil, and M. Mair (2014), EGU General Assembly 2014, Geophysical Research Abstracts, Vol. 16, EGU2014-13751, 2014.

Haddad, M. A., V. A. Rakov, and S. A. Cummer (2012), New measurements of lightning electric fields in Florida: Waveform characteristics, interaction with the ionosphere, and peak current estimates,J. Geophys. Res., 117, D10101.

Heidler, F. (1985), "Traveling current source model for LEMP calculation," in *Proc. 6th Int. Zurich Symp. Electromagn. Compat*., pp. 157-162.

Inan, U. S., S. A. Cummer, and R. A. Marshall (2010), A survey of ELF and VLF research on lightning‐ionosphere interactions and causative discharges, J. Geophys. Res., 115, A00E36.

Jacobson, A. R., X.-M. Shao, and R. Holzworth (2009), Full-wave reflection of lightning long-wave radio pulses from the ionospheric Dregion: Numerical model, J. Geophys. Res., 114, A03303.

Mur. G, "Absorbing boundary conditions for the finite-difference approximation of the time-domain electromagnetic-field equations," IEEE Trans. Electromagn. Compat., vol. EMC-23, no. 4, pp. 377–382, Nov. 1981.

Nickolaenko, A. P., A. Pavlovich, and M. Hayakawa (2002), Resonances in the Earth-ionosphere cavity. Vol. 19. Springer Science & Business Media.

Nucci, C. A., C. Mazzetti, F. Rachidi, and M. Ianoz (1988), On lightning return stroke models for LEMP calculations, paper presented at 19th International Conference on Lightning Protection, Graz, Austria.

Nucci, C. A., and F. Rachidi (1989), Experimental validation of a modification to the Transmission Line model for LEMP calculation, paper presented at

8th Symposium and Technical Exhibition on Electromagnetic Compatibility, Zurich, Switzerland.

Pichler, H., G. Diendorfer, and M. Mair (2010), Some parameters of correlated current and radiated field pulses from lightning to the Gaisberg tower, IEEJ Trans. Electr. Electron. Eng., 5(1), 8–13, doi:10.1002/tee.20486.

Rachidi, F., and C. A. Nucci (1990), On the Master, Uman, Lin, Standler and the modified transmission line lightning return stroke current models, Journal of Geophysical Research: Atmospheres (1984–2012), 95(D12), 20389-20393, doi:10.1029/JD095iD12p20389.

F. Rachidi, "Modeling Lightning Return Strokes to Tall Structures: A Review", Journal of Lightning Research, Vol. 1, pp. 16-31, 2007.

Romero, C., M. Paolone, M. Rubinstein, F. Rachidi, A. Rubinstein, G. Diendorfer, W. Schulz, B. Daout, A. Kaelin, and P. Zweiacker (2012), A system for the measurements of lightning currents at the Säntis Tower, Elect. Power Syst. Res. J., vol. 82, pp. 34–43.

Romero, C., F. Rachidi, M. Paolone, and M. Rubinstein (2013), "Statistical Distributions of Lightning Currents Associated With Upward Negative Flashes Based on the Data Collected at the Säntis (EMC) Tower in 2010 and 2011," Power Delivery, IEEE Transactions on, vol. 28, pp. 1804-1812.

Somu, V. B, V. A. Rakov, M. A. Haddad and S. A. Cummer (2012), Ionospheric reflection heights for wideband electric fields produced by consecutive return strokes within the same lightning flash, Abstract AE43A-0241, presented at 2012 fall meeting, AGU, San Francisco, Calif., December 3–7.

Thévenot, M., Bérenger, J. P., Monedière, T., and Jecko, F. (1999). A FDTD scheme for the computation of VLF-LF propagation in the anisotropic earth-ionosphere waveguide. In Annales des télécommunications ,Vol. 54, No. 5-6, pp. 297-310. Springer-Verlag.